

Accepted Manuscript

Title: Development and characterization of benzimidazole nano- and microparticles: A new tool for pediatric treatment of Chagas disease?

Authors: Katia P. Seremeta, Eva C. Arrúa, Nora B. Okulik, Claudio J. Salomon



PII: S0927-7765(19)30038-4
DOI: <https://doi.org/10.1016/j.colsurfb.2019.01.039>
Reference: COLSUB 9965

To appear in: *Colloids and Surfaces B: Biointerfaces*

Received date: 5 November 2018
Revised date: 11 January 2019
Accepted date: 19 January 2019

Please cite this article as: Seremeta KP, Arrúa EC, Okulik NB, Salomon CJ, Development and characterization of benzimidazole nano- and microparticles: A new tool for pediatric treatment of Chagas disease?, *Colloids and Surfaces B: Biointerfaces* (2019), <https://doi.org/10.1016/j.colsurfb.2019.01.039>

This is a PDF file of an unedited manuscript that has been accepted for publication. As a service to our customers we are providing this early version of the manuscript. The manuscript will undergo copyediting, typesetting, and review of the resulting proof before it is published in its final form. Please note that during the production process errors may be discovered which could affect the content, and all legal disclaimers that apply to the journal pertain.

Development and characterization of benznidazole nano- and microparticles: A new tool for pediatric treatment of Chagas disease?

Katia P. Seremeta ^{a,b}, Eva C. Arrúa ^{c,d}, Nora B. Okulik ^{a,b}, Claudio J. Salomon ^{c,d,*}

^a Departamento de Ciencias Básicas y Aplicadas, Universidad Nacional del Chaco Austral, Cte. Fernández 755, 3700, Pcia. Roque Sáenz Peña, Chaco, Argentina.

^b Consejo Nacional de Investigaciones Científicas y Técnicas (CONICET), Pcia. Roque Sáenz Peña, Chaco, Argentina

^c Instituto de Química Rosario, Consejo Nacional de Investigaciones Científicas y Técnicas (IQUIR-CONICET), Suipacha 531, 2000, Rosario, Argentina

^d Área Técnica Farmacéutica, Departamento de Farmacia, Facultad de Ciencias Bioquímicas y Farmacéuticas, Universidad Nacional de Rosario, Rosario, Argentina

*Corresponding autor at: Instituto de Química Rosario, Consejo Nacional de Investigaciones Científicas y Técnicas (IQUIR-CONICET), Suipacha 531, 2000, Rosario, Argentina. Tel.: +54 341 4804592; Fax: +54 341 4370477.

E-mail addresses: csalomon@fbioyf.unr.edu.ar, claudiosalomon@hotmail.com

(C.J. Salomon).

Statistical summary of the article

Total number of words: 5900

Tables/figures: 9 (1 Supplementary)

Graphical abstract.



Highlights

- Benznidazole nano/microparticles were obtained by freeze/spray-drying, respectively.
- Benznidazole nanoparticles were obtained in size range of 200-300 nm.
- Benznidazole microparticles exhibited a size range between 0.87 and 1.26 μm .
- Particle size of the nanoformulations did not changed after freeze-drying technique.
- Drug release from nano/microparticles was higher in comparison with untreated drug.

ABSTRACT

Benznidazole (BNZ) is the drug of choice for the treatment of Chagas disease in many countries. However, its low water solubility produces low and/or variable oral bioavailability. Thus, the aim of this work was to formulate micro- and nanoparticles based on Eudragit® RS PO and Eudragit® RL PO as a convenient approach to increase the dissolution rate of BNZ. The microparticles were obtained by means of spray-drying process while the nanoparticles were prepared through the nanoprecipitation technique and further freeze-drying. The results indicated that nanoparticles were obtained in 86% yield while microparticles were obtained in 68% yield. In both cases, the encapsulation efficiency of particles was greater than 78% while drug loading capacity was nearly 24% w/w and 18% w/w, after spray-drying and freeze-drying procedures, respectively. Images of scanning electron microscopy showed that the particles obtained by spray-drying and freeze-drying were in the micrometer and nanometer scale, respectively. FT-IR spectra of BNZ-loaded particles obtained by both methods showed characteristic bands of BNZ confirming that part of drug remained on their surface. Thermal analysis revealed that the drug crystallinity after both methods decreased. Physical stability evaluation of the nanoparticles confirmed that Pluronic® F68 was suitable to keep the particles size in a range of 300 nm after 70 days storage at 4 ± 2 °C. *In-vitro* release studies showed increased dissolution rate of drug from the particles obtained by both methods respect to untreated BNZ. The kinetics of drug release in acid media followed the Higuchi kinetics indicating drug diffusion mechanism from particles.

Keywords: Eudragit® RS PO, Eudragit® RL PO, dissolution efficiency, drug diffusion, benznidazole.

1. Introduction

Chagas disease, caused by the protozoan parasite *Trypanosoma cruzi* (*T. cruzi*) affects about 6 to 7 million people worldwide, mainly in Latin America [1]. Even though the disease was discovered more than hundred years ago, to these days there are only two drugs, nifurtimox and benznidazole (BNZ), to treat it [2]. BNZ is currently considered the trypanocidal drug of choice because of its better tolerability profile and possibly efficacy [3]. In particular, it is highly effective during the acute phase of the infection and in chronically infected children [4]. Moreover, BNZ treatment is recommended in congenital cases and reactive infections among all children and for patients up to 18 years old in the indeterminate chronic phase [5]. It is worth noting that, recently, BNZ was approved by FDA to treat patients 2-12 ages [6]. The etiological treatment is useful to prevent congenital infection by *T. cruzi*. Fabbro et al. showed that the relative risk of transmitting the infection is 25 times higher for untreated mothers than for those who received treatment before pregnancy [7]. However, it is important to highlight that BNZ, the first-line drug in the treatment of Chagas disease, it is practically insoluble in water (0.4 mg/mL) and, as a consequence, its solubility and dissolution rate may compromise the further chemotherapeutic performance [8,9]. To overcome such drawbacks, the administration of higher doses may be needed, resulting in the appearance of adverse effects [1,10]. Accordingly, treatment with BNZ is commonly discontinued in as much as 20% of cases due to the well-known side effects [11]. As a consequence, novel delivery systems are urgently needed to improve the biopharmaceutical properties of BNZ in order to find a suitable


treatment for Chagas disease. In the last years, novel BNZ formulations have been developed including co-solvent systems [12], polymeric solid dispersions [13-15], microparticles [16] and complexation with cyclodextrin derivatives [17-19]. In addition, as reviewed by Romero and Morilla, several nanosystems to treat Chagas disease were developed by using different carriers. Physicochemical properties of such formulations were discussed to determine their *in-vitro* and *in-vivo* efficacy [20]. In particular, BNZ nanoformulations including liposomal formulations [21-24], nanocrystals [25,26] and polymeric nanoparticles [27] were described in the last years. However, the only chemotherapeutic treatment available for Chagas disease, to these days, is based on tablets, an unsuitable dosage form to treat neonates and young children [28]. BNZ was developed and produced as tablets by Roche until 2011 when production was discontinued. Then, this production was taken up by the Brazilian Pharmaceutical Laboratory of the State of Pernambuco (LAFEPE) and ELEA Laboratory (Argentina) [4]. ELEA Laboratory formulated BNZ into tablets of 50 and 100 mg (ABARAX®). Until recently, the 50 mg tablets were the only formulation available for children. Later, as a result of an alliance between the Drugs for Neglected Diseases initiative (DNDi) and LAFEPE, a pediatric dosage form (BNZ 12.5 mg tablets) was developed and a corresponding clinical trial (ClinicalTrials.gov Identifier: NCT01549236) was conducted in children weighing <20 kg. This pediatric formulation was registered in Brazil and in 2013 was included on the WHO's Essential Medicines List for children as a new dosage form indicated for children below 2 years old with Chagas disease [5,29,30]. However, in many occasions the pediatric population is still treated by fractioning those tablets according to the body weight of each patient. As reported, such manipulations may result in the

administration of sub-therapeutic or toxic doses [31]. In addition, both the stability and bioavailability of BNZ may be greatly reduced. In this regard, multi-particulate formulations may represent an attractive alternative for children below the age of 6, as recommended by WHO [32]. These types of pharmaceutical dosage forms can be administered into the buccal cavity of the children or mixed with beverages before administration [33]. Therefore, in this study, multi-particulate systems based on Eudragit® RS PO and Eudragit® RL PO and loaded with BNZ were developed. BNZ nanoparticles were obtained by freeze-drying while BNZ microparticles were obtained by spray-drying. The solid state characterization of both nano- and microparticles was performed by means of thermal analysis (DSC), infrared spectroscopy (FT-IR) and scanning electronic microscopy (SEM). The influence of storage conditions on long-term stability of BNZ nanoparticles was evaluated at different temperatures in solution and also in a solid state. In addition, the release profile for each multi-particulate system was investigated.

2. Materials and methods

2.1. Materials

BNZ (lot 9978 A; Laboratorio Elea, Buenos Aires, Argentina) was provided by Instituto Nacional de Parasitología, ANLIS Malbrán, Ministerio de Salud de la Nación (Buenos Aires, Argentina). Eudragit® RL PO and Eudragit® RS PO (copolymers of ethylacrylate, methylmethacrylate and methacrylic acid esterified with quaternary ammonium groups) and Sipernat® (specialty silica) were kindly donated by Evonik (Argentina). Pluronic® F68 (actually called Kolliphor® P188), a

nonionic surfactant, was kindly donated by BASF (Argentina). All the other reagents and chemicals were of analytical grade and used as received. 

2.2. Preparation of BNZ nanoparticles

BNZ-loaded nanoparticles (NP) were prepared by nanoprecipitation and freeze-drying. Firstly, pure polymer (Eudragit[®] RL PO or Eudragit[®] RS PO) or blend (Eudragit[®] RL PO/Eudragit[®] RS PO, 1:1 weight ratio) (0.025 g total weight) and BNZ (0.01 g) were dissolved in acetone (10 mL) (polymer:drug weight ratio 2.5:1); whereas that Pluronic[®] F68 (0.01875 g) was dissolved in distilled water (20 mL). The organic phase was injected on the aqueous phase using a syringe (10 mL) and needle (21G1, 0.80x25 mm) at constant flow rate (20 mL/h, Pump 11 Elite Infusion/Withdrawal Programmable Single Syringe, Harvard Apparatus, U.S.). The aqueous phase was maintained under moderate magnetic stirring (200 rpm) (IKA[®] C-MAG HS 7 digital, Germany). The resulting suspension was stirred at room temperature under fume hood for 8 h to allow the complete evaporation of the organic solvent. The suspension obtained was filtered through filter paper and the supernatant was frozen at -20 °C and freeze-dried (Freeze-Dryer RIFICOR model L-I-E300-CRT, Argentine) for 48 h. Powder obtained was stored at room temperature protected from light and moisture until use. Three formulations of NP were obtained in triplicate using Eudragit[®] RL PO, Eudragit[®] RS PO and the corresponding blend (1:1 weight ratio). These were namely NP-RL, NP-RS and NP-RL/RS, respectively. Blank particles (without BNZ) were prepared and used as references.

2.2.2. Preparation of BNZ microparticles

BNZ-loaded microparticles (MP) were obtained by suspension and spray-drying. Firstly, Eudragit® RL PO, Eudragit® RS PO or blend (Eudragit® RL PO/Eudragit® RS PO, 1:1 weight ratio) (6.0 g total weight) and BNZ (2.4 g) were dissolved in absolute ethanol (60 mL) under moderate magnetic stirring (IKA® C-MAG HS 4 digital, Germany) overnight. The polymer:drug weight ratio was 2.5:1. Then, this organic phase was added to a dispersion of Sipernat® (7.5% w/v) in distilled aqueous (540 mL) and left under magnetic stirring for 1 h. The sample was homogenized using a T18 Ultra-Turrax (IKA®-Werke GmbH & Co.KG) (17,500 rpm, 5 min). The suspension resulting was maintained throughout the process under constant magnetic stirring (200 rpm) (IKA® C-MAG HS 4 digital, Germany) to ensure homogeneity while was fed into a Mini Spray Dryer Büchi B-290 (Büchi Labortechnik AG, Switzerland) through a two-fluid nozzle (0.70 mm inner diameter) in open-loop mode and co-current flow. The operating conditions were the following: air inlet temperature of 130 °C, atomizing air flow rate of 600 L/h, liquid flow rate of 1 mL/min, carrier gas flow rate (aspirator) of 35 m³/h and pressure of 4 bar. The resulting air outlet temperature was 65 °C. The dried powder was recovered from the glass collection vessel and weighed to determine the yield. Then, MP were stored in glass vials at room temperature protected from light and moisture until use. Three formulations of MP were obtained in triplicate using Eudragit® RL PO, Eudragit® RS PO and blend (1:1 weight ratio). These were namely MP-RL, MP-RS and MP-RL/RS, respectively. In addition, blank particles were also prepared.

2.3. Characterization of BNZ-loaded particles

2.3.1. External morphology

The external morphology of BNZ-loaded particles was visualized by scanning electron microscopy (SEM, JEOL JSM-5800LV Scanning Microscope, USA) operating at an accelerating voltage of 15 kV. Samples were previously sputter-coated with a gold layer to make them conductive (Denton Vacuum, Desk II).

2.3.2. Size and size distribution

2.3.2.1. BNZ nanoparticles

Size, size distribution and zeta potential of the NP were determined, before and after freeze-drying, by dynamic light scattering (DLS) using a NanoPartica SZ-100 Horiba instrument (HORIBA Instruments Inc. California, USA). Measurements were conducted at a scattering angle of $\theta = 173^\circ$ to the incident beam and at 25 °C. Results of size (intensity mean hydrodynamic diameter, D_h), size distribution (polydispersity index, PDI) and zeta potential (Z-pot) are expressed as mean \pm S.D. of three independent samples. To evaluate the influence of the freeze-drying process on the D_h , NP (0.01 g) were dispersed in an aqueous solution of Tween[®] 80 (0.1% w/v, 15 mL), sonicated (10 min) and analyzed by DLS. The factor of variation of the D_h (f_s) was determined by Equation (I):

$$f_s = \frac{S_f}{S_i} \quad (I)$$

Where S_f and S_i is the D_h of the NP after and before the freeze-drying process, respectively. The results are expressed as mean \pm standard deviation (S.D.) of three independent samples prepared under the same conditions.

2.3.2.2. BNZ microparticles

Size and size distribution of the MP were estimated by SEM. Images with 20X magnification were analyzed with an image analysis system (Image Pro-plus® software 6.0) to obtain the average size value of these MP.

2.3.3. Yield, loading capacity and entrapment efficiency

The yield (%) after freeze-drying and spray-drying processes was determined using the Equation (II):

$$\text{Yield (\%)} = \frac{W_p}{W_0} \times 100 \quad (\text{II})$$

Where W_p is the total weight of BNZ-loaded particles obtained after drying process and W_0 is the total initial weight of polymers, excipients and BNZ employed in their preparation.

To determine the loading capacity (%LC) and the encapsulation efficiency (%EE), BNZ-loaded particles (0.01 g) of each sample were dissolved in absolute ethanol/distilled water (97/3 v/v) (5 mL) under magnetic stirring during 30 min. Then, an aliquot of this suspension (200 μ L) was diluted with the same solvent up to a final volume of 5 mL. The BNZ concentration was determined by UV-visible spectrophotometry ($\lambda = 324$ nm, UV-1800 Shimadzu UV-VIS Spectrophotometer, Japan) at 25 °C using a calibration curve in the range of 5-

40 $\mu\text{g/mL}$ in ethanol/distilled water (97/3 v/v) ($R^2 > 0.9997$). Measurements were performed in triplicate and results are expressed as mean \pm S.D.

The %LC of the BNZ-loaded particles was calculated according to Equation (III):

$$\%LC = \frac{W_{BNZ}}{W_P} \times 100 \quad (\text{III})$$

Where, W_{BNZ} is the weight of BNZ in the particles and W_P is the total weight of BNZ-loaded particles obtained.

The %EE of the particles was determined according to Equation (IV):

$$\%EE = \frac{LC_P}{LC_T} \times 100 \quad (\text{IV})$$

Where LC_P and LC_T are the experimental and theoretical loading capacity of the BNZ-loaded particles, respectively.

2.3.4. Attenuated total reflectance/Fourier transform-infrared spectroscopy (ATR/FT-IR)

ATR/FT-IR spectroscopy is a fast and versatile technique for determining interactions between BNZ and the corresponding polymers. Therefore, free BNZ, blank particles and BNZ-loaded particles obtained by both methods were analyzed by FT-IR (Nicolet iS5 FT-IR spectrometer, Thermo Scientific, USA) equipped with ATR (iD3 ATR, Thermo Scientific, USA) in the range between 4000 and 600 cm^{-1} (16 scans, spectral resolution of 4.0 cm^{-1}). FT-IR spectra were obtained using the OMNIC 8 spectrum software (Thermo Scientific, USA).

2.3.5. Thermal analysis

The thermal analysis of free BNZ, polymers and BNZ-loaded particles was performed by differential scanning calorimetry (DSC, Model PT 1000 differential scanning calorimeter, Germany). Samples (~5 mg) were loaded to aluminium pan, crimped, sealed and heated in a simple heating temperature ramp from 25 to 200 °C at a rate of 10 °C/min under dry nitrogen atmosphere (flow rate 100 mL/min). The different thermal transitions were analyzed. The crystallinity degree (%C) of BNZ ($\%C_{BNZ}$) in the different particles was calculated according to Equation (V):

$$\%C_{BNZ} \frac{\Delta H_{m-BNZ}}{\Delta H^c_{m-BNZ}} \times 100\% \quad (V)$$

Where ΔH_{m-BNZ} is the value of melting enthalpy of BNZ in the particles and ΔH^c_{m-BNZ} is the value of melting enthalpy of 100% crystalline BNZ. Values were normalized to the content of each one of the components in the particles.

2.4. Physical stability studies

According to ICH guidelines, the NP were stored in closed vials, protected from light, in a refrigerator (4 ± 2 °C) and in a close cupboard (25 ± 2 °C). The samples were evaluated in terms of particle size at 0, 7, 14, 21, 28, 35, 42, 56, 63, and 70 days, respectively, and Z-pot at 0 and 70 days. All determinations were carried out in triplicate and the mean values and S.D. are reported (see 2.3.2.1.).

2.5. In-vitro drug release studies

The release of BNZ from the formulated NP and MP was carried out by using the dialysis bag method such as other published works with minor modifications [34]. For comparison, the release of untreated BNZ was also analyzed. Each sample containing 5 mg of BNZ was dispersed in 0.1 N HCl (pH 1.2, 10 mL). The resulting suspension was placed into a dialysis bag (regenerated cellulose tubing, molecular weight cut off = 12,000–14,000 g/mol) and placed in a beaker containing the release medium (0.1 N HCl, 100 mL). This volume of medium ensures sink conditions. System was maintained at 37 ± 1 °C under moderate magnetic stirring (200 rpm). At predetermined time intervals (10, 15, 20, 30, 45, 60, 90, 120, 180, 240, 300, 360, 420 and 480 min) an aliquot of the release medium (4 mL) was withdrawn and it was replaced by fresh medium pre-heated at 37 °C to maintain sink conditions. The dissolved BNZ amounts in samples were quantified directly or by dilution with 0.1 N HCl using UV-visible spectrophotometer set to 324 nm (see 2.3.3.). Assays were carried out in triplicate and the results are expressed as mean \pm S.D. The dissolution profiles were compared using the dissolution efficiency (DE) value at 30 min (DE_{30}), 60 min (DE_{60}) and 120 min (DE_{120}). Statistical analysis of the DE was performed using a one-way analysis of variance (ANOVA) followed by least significant difference using GraphPad Prism version 5.00 for Windows (GraphPad Software, Inc., USA).

2.5.1. Kinetic of release

Modeling and comparison of drug release profiles was conducted with DDSolver program and Microsoft® Excel 2007. Two different models were used for

describing the release mechanism of BNZ from the particles, Higuchi model and Korsmeyer-Peppas model:

Higuchi model

$$F = k_H \cdot t^{0.5} \quad (\text{VI})$$

Where F is percentage of drug released and k_H is the Higuchi release constant. The release rate is explained as a square root of the time-dependent process based on the Fickian diffusion.

Korsmeyer–Peppas model

$$F = k_{KP} \cdot t^n \quad (\text{VII})$$

Where k_{KP} is the release constant incorporating structural and geometric characteristics of the drug dosage form and n is the diffusional exponent indicating the drug release mechanism. The criterion for selecting the most appropriate model was based on a goodness-of-fit test.

3. Results and discussion

3.1. Characterization of BNZ nanoparticles

As mentioned above, BNZ is practically insoluble in water (0.4 mg/mL) and, as a consequence, higher oral doses may be required to achieve a therapeutic drug concentration in the systemic circulation. Therefore, it is of utmost importance to explore if other alternatives based on the formulation of BNZ polymeric

nano/microparticulate systems may improve its solubility and dissolution [10]. One of the most widely applied techniques to formulate nanoparticulate systems is the nanoprecipitation or solvent displacement method. It is based on the interfacial precipitation on the nanoscale of a polymer after displacement of a semi-polar solvent, miscible with water from a lipophilic solution [35]. This methodology has been widely applied to obtain particles in the 100-300 nm range. It is mostly suitable for encapsulation of hydrophobic compounds that are soluble in ethanol or acetone [35]. These non-halogenated organic solvents are less toxic and more eco-friendly than halogenated organic solvents used in other encapsulation methods as the emulsion/solvent evaporation [27,36,37]. As carrier for the development of NP were selected Eudragit® RS PO and Eudragit® RL PO polymers. These polymers are amorphous, non-biodegradable, nonabsorbable, and nontoxic. In addition, cationic Eudragit® derivatives may interact with the negatively charged intestinal mucosa after the oral administration of Eudragit®-based drug delivery systems [16,38]. Thus, BNZ and the corresponding polymers were dissolved in acetone (solvent) and added to a water/Pluronic® F68 solution (non-solvent). After the diffusion of acetone into the non-solvent phase, it was observed the appearance of a white precipitate suggesting that both the polymer and the hydrophobic BNZ became insoluble in contact with the non-solvent phase. In general, the nanoprecipitation is a process of high surface energy and, as a consequence, the newly formed nanoparticles may be agglomerated. Thus, Pluronic® F68 was used as steric stabilizer. The selection of this surfactant was based on previous reports that showed that smaller nanoparticles were obtained using Pluronic® F68 in comparison with Pluronic® F-127 and poly(vinyl alcohol) [39]. Once obtained the BNZ

nanosuspension, a solidification technique as freeze-drying was applied to obtain the corresponding powder. Solid form is more desirable than liquid form, as reaction rates of physical and chemical interactions are slower in solid state. However, freeze-drying often produces changes on nanoparticle properties, which may affect its size due to particle aggregation under cryogenic stress condition and compression during the formation of ice crystals in the internal water phase [40]. Thus, a cryo-protectant may be needed to inhibit interactions between nanoparticles during the freezing process and thus preserve redispersibility [41]. However, Pluronic[®] F68, an ABA triblock copolymer consisting of hydrophilic polyoxyethylene (PEO) and hydrophobic polyoxypropylene (PPO), is a stabilizer that can prevent the agglomeration of the particles during freeze-drying [42]. In this regard, Lee and Lin [43] assayed the effects of different surfactants (HCO-60, sodium dodecyl sulfate, Tween[®] 80, PEG 400, Pluronic[®] F68, and Pluronic[®] F127) on the conformational stability and structural similarity of a hormone in lyophilized forms. The results indicated the most optimal stabilization effect of Pluronic[®] F68. This effect might be attributed to its ability to protect hormone from dehydration and thermal stresses during lyophilization due to it is a much larger molecule with longer hydrophilic and hydrophobic chains is thought to play an important role to prevent the interfacial induced adsorption [43]. Herein, the stirring speed (200 rpm) at room temperature was found to be enough to prepare NP in a range of 200-300 nm with narrower size distribution.

According to the literature, an increased particle size after lyophilization is frequently observed [44,45]. However, in this study the results of DLS analysis showed that the freeze-drying process did not greatly modify the particle size of

prepared nanosystems. Thus, the range of the sizes of D_h , before and after freeze-drying of NP, were found to be around 201-250 nm and 242-281 nm, respectively (**Table 1**). The increase in particle sizes after freeze-drying was tiny with f_s value of around 1, demonstrating the freeze-drying process did not lead to significant NP aggregation (**Table 1**). Regarding size distribution, PDI value in the range of 0.15-0.3, indicates size homogeneity for submicron particles. Thus, all formulations showed PDI value below 0.2 before and after freeze-drying, indicating size homogeneity (**Table 1**). In addition, surface charge of NP was determined by the Z-pot. It should be note that Eudragit® is positively charged due to the presence of quaternary ammonium groups. Therefore, all formulations showed positive Z-pot values from +24 to +37 mV before and after freeze-drying (**Table 1**). These results are agreement with the literature [27,46,47]. The high charges can prevent aggregation by repulse particles with each other due to electrostatic stabilization induced by the cationic copolymer able to induce stable formulations [27]. Moreover, the positively charged NP could be attached to the negatively charged epithelial mucin layer in the gastrointestinal tract which in turn would improve drug oral bioavailability [48].

The shape and surface morphology of the NP were observed by means of SEM, a very useful technique to analyze particles > 100 nm with a resolution of 5 nm, collecting information related with the size, surface and shape [49]. As seen in **Fig. 1C**, BNZ raw material presented a prismatic form with crystals of variable sizes such as those observed by Palmeiro-Roldán et al. [50]. In contrast, NP were found to be in the nanometer scale (< 1 μm) and partially adhered by Pluronic® F68 during the freeze-drying process (**Fig. 1B**). It should be noted that BNZ

crystals (**Fig. 1 C**) were not visualized on the surface of the nanoparticulate system.

Insert Table 1.

3.2. Characterization of BNZ microparticles

On the other hand, and using the same cationic polymers, MP were prepared by means of spray-drying process. As known, it is, probably, the most convenient tool to encapsulate active materials within different types of carriers including biodegradable polymers [51]. It is an attractive alternative to conventional techniques since it is a single-step process, shorter and cheaper compared to other drying processes commonly used in industry such as freeze-drying, because it does not involve deep cooling, usually associated with great energy consumption. It is worth mentioning that, compared to freeze-drying, spray-drying is up to 30-50 times cheaper [52,53]. The analysis of MP was performed using Image Pro-plus® software 6.0. As seen in **Fig. 1A**, spherical particles in a micrometer scale with a smooth surface were obtained. Media size of MP-RL, MP-RS and MP-RL/RS was $0.87 (\pm < 0.01) \mu\text{m}$, $1.08 (\pm 1.16) \mu\text{m}$ and $1.26 (\pm < 0.01) \mu\text{m}$, respectively. These results are in agreement with the findings of the previous studies. Thus, Rabbani and Seville [54], who produced dry powders suitable for inhalation containing β -estradiol by spray-drying using a Mini Spray Dryer B-290 with a 0.7 mm two-fluid nozzle. The mean particle size of the resultant microparticles was between 2.5 and 7 μm , making them suitable pulmonary administration [54]. In addition, Ní Ógáin et al. [53] described the formulation of less than 2 μm trypsin-loaded microparticles for pulmonary delivery

using the same drying equipment [55]. On the other hand, García et al. [56] developed chitosan-pectin-carboxymethylcellulose microspheres by spray-drying to improve the oral absorption of albendazole as a model drug. The mean diameter of the microspheres was 2.8 μm [56].

Insert Figure 1.

3.3. Yield, loading capacity and entrapment efficiency

The production yields obtained during the formulation process were nearly 86% for NP (**Table 1**). In agreement with the bibliography, nanoprecipitation is one of the most suitable techniques to prepare solid colloidal particles in the range of nanometer [57]. In this study, the selection of the polymers and stabilizer, the stirring speed and the freeze-drying process confirmed the robustness of the methodology to obtain NP in high yield [34,39]. On the other hand, spray-drying process exhibit several advantages over other solvent evaporation procedures, as already described. However, one of the main challenges of such process is the moderate yield obtained on the laboratory scale (20-70%) when conventional dryers are used [58-60]. In this work, MP were obtained in a 68%, approximately (**Table 1**). This moderate yield could be due to the powder tend to adhere to the glass wall of cyclone, as observed during the drying process [59]. This is consistent with the work of Rassau et al. [61] who informed yields nearly 60% during the preparation microparticles based on Eudragit® and loaded with ketoprofen. Another key parameter during the incorporation of drugs into polymeric particles is the %EE. Usually, it is based on the selected encapsulation technique, polymer type and concentration and drug-polymer weight ratio.

Herein, regardless of the preparation method and the polymeric composition the %EE was high on all formulations (> 78.8%), as seen in **Table 1**. This is consistent with the literature data due to both nanoprecipitation/freeze-drying and spray-drying can yield high %EE of lipophilic drugs within polymeric carriers [62,63]. Moreover, %LC values were around 20% (18% and 23% in NP and MP, respectively) indicating a moderate drug loading capacity of all systems (**Table 1**). In this regard, a considerable amount of NP or MP would be needed to deliver the required dose in order to achieve the desired pharmacological activity. However, the enhancement of BNZ dissolution rate (**Fig. 3**) may lead to improve the oral bioavailability and, therefore, lower doses of BNZ might be administered, minimizing its adverse effects. [8]. In any case, to confirm this postulate, it is necessary to evaluate the *in-vivo* performance of such formulation in comparison with the non-encapsulated drug.

3.4. Solid state characterization of the BNZ-loaded particles

3.4.1 Attenuated total reflectance/Fourier transform-infrared spectroscopy (ATR/FT-IR)

To analyze the potential interactions between groups of BNZ with the backbone of Eudragit® after both encapsulation processes, the samples of the different BNZ-loaded particles were studied by ATR/FT-IR spectroscopy and compared to the spectrum of blank particles and free BNZ. Blank particles showed characteristic bands of pure polymers (**Figure 1S**). Free BNZ showed the characteristic bands of (i) NH deformation at 1565 cm^{-1} , characteristic of an amide II, (ii) carbonyl stretching (amide I) at 1685 cm^{-1} and (iii) C-N stretching at

1318 cm^{-1} . The band due to stretching vibrations of N-H is at 3,330 cm^{-1} . In addition, the cluster of bands at 3180, 3160, 3120, 3090 and 3000 cm^{-1} suggests symmetrical and asymmetrical stretching vibrations for the methylene in the benzyl group and stretching of the aromatic C-H [18] (Figure 1S). Regarding the NP and MP, the intensity and shape of the bands between 1600 and 1000 cm^{-1} did not exhibit significant modifications (Figure 1S). However, a significant reduction of relative intensity of the peaks in the region of 3300-3000 cm^{-1} was clearly detected. It could be due to the formation of H-bonding between the N-H group of BNZ and the C=O group of the polymer. These findings are in agreement with those results reported by Lima et al. [14] and dos Santos-Silva et al. [27], who showed similar modifications of the FT-IR spectra of BNZ by interactions with other polymers [14,27].

3.4.2 Thermal analysis

DSC is a good standard technique to elucidate the crystalline or amorphous nature of drugs associated at a polymeric matrix after an encapsulation process. All the BNZ-loaded particles showed a characteristic glass transition temperature (T_g) of Eudragit® at 49-50 °C, the thermal behavior being identical to that of pure polymer [64] (Table 2). The thermogram of BNZ showed an endothermic peak at 195 °C ($\Delta H_m = 118.4 \text{ J/g}$) that was considered as 100% crystallinity, as reported in the literature [14,65]. BNZ-loaded particles obtained by both methods exhibited the T_m of BNZ at 195-197 °C with $\%C_{BNZ} < 25\%$ in all cases, suggesting that the drug underwent partial amorphization in polymeric matrix during the encapsulation process (Table 2). These data are in agreement with the work of García et al. [16], who described a similar thermal event of BNZ after the

formation of polyelectrolyte complexes with other polymethacrylate derivatives [16].

Insert Table 2.

3.5. Physical stability studies

The physical stability of a nanosystem is of particular interest when the solution is freeze-dried [66]. Thus, in this study, the particle size of the nanoformulations was evaluated before and after drying processes over a period of 70 days, at both 4 ± 2 °C and 25 ± 2 °C (**Fig. 2**). As seen in **Fig. 2A** and **Fig. 2B**, a size change was observed in the NP placed at room temperature. In solution, the particle size increased up to nearly 920 nm using Eudragit® RS PO as a carrier from its original size, around 200 nm (**Fig. 2A**). After freeze-drying, the analysis of the nanosystems revealed that the NP were in the size range of 650 to 750 nm (**Fig. 2B**). This finding might be attributed, mainly, to an increased interaction of the NP under storage at room temperature, probably due to an incomplete coverage of the NP surfaces by means of the stabilizer leading, as a consequence, to the formation of new agglomerates. In this regard, Reddy et al. [67] found that particle size of tamoxifen citrate-loaded nanoparticles increased under storage at 50 °C during 30 days, as a result of particle aggregation [67]. On the other hand, it was observed that NP placed in solution at 4 ± 2 °C changed its particle size from around 200 nm (0 day) to 400 nm (70 days), depending the type of polymer (**Fig. 2C**). It could be related, probably, to the phenomena of crystal growth and/or the formation of aggregates in solution. In contrast, freeze-dried nanosystems displayed the best stability (**Fig. 2D**). Thus, NP formulated with Eudragit® RL PO, Eudragit® RS PO or Eudragit® RL PO/Eudragit® RS PO (1:1 w/w) exhibited a

particle size of 301.9 nm, 242.4 nm, and 282.4 nm, respectively at 0 days while at 70 days the particle size was 320.9 nm, 270.5 nm, and 303.4 nm, respectively (**Fig. 2D**). Clearly, under this storage condition, NP exhibited a stable behavior, probably related with the absence or a very small influence of the Ostwald ripening [68]. It is worth mentioning that Quintanar-Guerrero et al. [69] described an aggregation of poly(D,L-lactic acid) nanoparticles, after freeze-drying, by using Pluronic® F68 as stabilizer. However, in this case such polymer was able to stabilize the NP under storage, at least for 70 days. Therefore, it could be suggested that Pluronic® F68 is a convenient approach to avoid agglomeration when freeze-dried samples are placed at 4 ± 2 °C and then dispersed in water. From the data obtained, it can be suggested that NP placed at low temperature are more stable, in terms of particle size, than the corresponding NP placed at room temperature, regardless of the Eudragit® used. On the other hand, the Z-pot values slightly changed after 70 days placed at both 4 ± 2 °C and 25 ± 2 °C, indicating that the NP surface was not greatly modified after freeze-drying process suggesting that these data are not related to the particle size stability results.

Insert Figure 2.

3.6. In-vitro drug release

Release studies were performed in HCl 0.1 N (pH 1.2) at 37 °C to simulate the pH gastric physiological due to these particles were formulated to be orally administered. As compared to the raw BNZ, the results showed enhanced BNZ dissolution rate from particles obtained by both methods (**Fig. 3**). MP showed

similar profiles in the three formulations and differences were not statistically significant ($p > 0.05$) (**Fig. 3A**). As seen in **Table 3**, DE_{30} , DE_{60} and DE_{120} values of MP were greater than non-encapsulated BNZ. Differences were statistically significant ($p < 0.001$) (**Table 3**). This could be due to that part of BNZ remained on the surface of the MP, according to SEM image (**Fig. 1A**) and FT-IR spectra, leading to a rapid release and after dissolution of BNZ in the medium of similar gastric pH (**Fig. 3A**). NP also showed dissolution profile higher than free-BNZ (**Fig. 3B**) with DE_{30} , DE_{60} and DE_{120} values greater than non-encapsulated BNZ. Differences were statistically significant ($p < 0.001$) (**Table 3**). In comparison with these findings, other researchers obtained promising results using liposomal formulations with the purpose of increasing the amount of BNZ delivered to infected Kupffer cells, which naturally phagocytose multilamellar liposomes. Such formulations were prepared by employing hydrogenated phosphatidylcholine from soybean (HSPC): Cholesterol (Chol): distearoyl-phosphatidylglycerol (DSPG) (molar ratio 2:2:1) as lipid matrix [21,23]. The drug loading obtained was of 2 g BNZ/100 g total lipids at a total lipid concentration of 20-30 mM. *In-vitro* release of drug after 60 min at 450-fold dilution in buffer at 37 °C showed that the amount of drug associated to liposomes was reduced from 2 to 0.25 g BNZ/100 g total lipids at a rate of 65% (drug lost) min^{-1} at the first minute followed by 0.4% (drug lost) min^{-1} for the next 59 min. In our study, the higher dissolution rate of drug from the particles could be due to the size reduction of the drug, increase of surface area and reduction of the drug crystallinity after processes [14,70] (**Table 2**). Thus, as the dissolution rate in the gastrointestinal tract of poor water-soluble drugs such as a BNZ often limits drug absorption and therefore the oral

bioavailability, enhanced dissolution could lead to an increase in BNZ oral bioavailability [19].

Insert Figure 3.

3.6.1. Kinetic of drug release

The calculated fitting parameters of the kinetic models after applying a non-linear regression analysis are summarized in **Table 3**. To reveal the release mechanism of BNZ from particles, the dissolution profiles were fitted by two different kinetic models: Higuchi and Korsmeyer-Peppas. The values of R^2_{adj} were higher for the Higuchi model (0.9458-0.9615) than Korsmeyer-Peppas (0.8350-0.9247) in all formulations (**Table 3**). The Higuchi model is an invaluable tool in developing a controlled drug delivery [71]. Higuchi was the first to derive an equation to describe the release of a drug from an insoluble matrix as the square root of a time-dependent process based on Fickian diffusion [72]. This equation addresses the release rate of a drug from a matrix, usually a polymer, where the loading of drug exceeds its solubility in the matrix into a surrounding fluid [71]. On the other hand, the Korsmeyer-Peppas model is widely used to indicate the appropriate release mechanism between different mechanisms [73]. In this model, n values ≤ 0.43 indicate that occurs Fickian diffusion. Conversely, if $n \geq 0.85$ the diffusion comprises super-Case II transport where the drug release is purely governed by polymer relaxation. Finally, if n is between these values (0.43 and 0.85), anomalous diffusion is predominant, i.e., non-Fickian diffusion process, where the release can be attributed to a combination of drug diffusion and polymer chain relaxation [74]. In our study, all the NP obtained by freeze-drying showed n values

in the 0.7016–0.7120 (**Table 3**) range indicating that the drug release could be accomplished by diffusion of the drug from matrix and polymer chain relaxation. On the other hand, the MP obtained by spray-drying showed n values ≥ 0.85 (0.8500-0.9721) (**Table 3**) indicating that the drug release could be produced by polymeric relaxation (Super Case II). In agreement with other reports dealing with the formulation of BNZ microparticles, in this work the best fitting to the Higuchi model indicates that the release of the drug from the particles was by diffusion from the polymer matrix.

Insert Table 3.

4. Conclusions

In this study, it was demonstrated for the first time that both nanoprecipitation/freeze-drying and suspension/spray-drying are effective methods to obtain BNZ nano- and microparticles, respectively, in relatively high yields. It is worth mentioning that BNZ nanoparticles were obtained within the size range of 200-300 nm and the stabilizer was able to keep the nanoparticle size and zeta potential during the freeze-drying process. In addition, the physical stability evaluation of the BNZ nanoparticles indicated that Pluronic® F68 was suitable to keep the particle size in a range of 300 nm after 70 days storage at 4 ± 2 °C. FT-IR studies of the BNZ particles suggested some interactions between the drug and the polymers while thermal analysis revealed that the drug crystallinity decreased after both freeze- and spray-drying procedures. All these factors allowed to enhance dissolution efficiency of BNZ from particles in comparison with the raw drug. The best fitting to the Higuchi model of dissolution

profiles indicates that the release of the drug from the particles was by diffusion from the polymer matrix. Thus, in agreement with urgent needs for Chagas disease pediatric treatments, all these formulations obtained in powder form would allow dose flexibility to suit the dosing requirements across all age groups. Taking in account these results, further *in-vitro/in-vivo* studies in animal infection model will be performed in the near future to analyze whether these polymeric multiparticulate BNZ formulations may exhibit a better biological activity in comparison with the raw drug.

Acknowledgments

The authors express their gratitude to the Universidad Nacional de Rosario (U.N.R., Rosario, Argentina), Universidad Nacional del Chaco Austral (UNCAUS, Chaco, Argentina), and Consejo Nacional de Investigaciones Científicas y Técnicas (CONICET, Argentina). KPS and ECA thank to CONICET for a postdoctoral and Ph.D. fellowship, respectively.

References

- [1] L.D. Tessarolo, R.R.P.P.B. de Menezes, C.P. Mello, D.B. Lima, E.P. Magalhães, E.M. Bezerra, F.A.M. Sales, I.L. Barroso Neto, M.F. Oliveira, R.P. Dos Santos, E.L. Albuquerque, V.N. Freire and A.M. Martins, *Parasitology* 12 (2018) 1.
- [2] C. Crespillo-Andújar, S. Chamorro-Tojeiro, F. Norman, B. Monge-Maillo, R. López-Velez and J.A. Pérez-Molina, *Clin. Microbiol. Infect.* S1198-743X (2018) 30465.
- [3] J.A. Pérez-Molina and I. Molina, *Lancet* 391 (2018) 82.
- [4] M.L. Fernández, M.E. Marson, J.C. Ramirez, G. Mastrantonio, A.G. Schijman, J. Altcheh, A.R. Riarte and F.G. Bournissen, *Mem. Inst. Oswaldo Cruz*, 111(2016) 218.
- [5] M.G. Davanço, M.L. Campos, T.A. Rosa, E.C. Padilha, A.H. Alzate, L.A. Rolim, P.J. Rolim-Neto and R.G. Peccinini, *Antimicrob. Agents Chemother.* 60 (2016) 2492.
- [6] K. Traynor, *Am. J. Health Syst. Pharm.* 74 (2017) 1519.
- [7] D.L. Fabbro, E. Danesi, V. Olivera, M.O. Codebó, S. Denner, C. Heredia, M. Streiger and S. Sosa-Estani, *PLoS Negl. Trop. Dis.* 8 (2014) e3312.
- [8] C.B.M. Figueirêdo, D. Nadvorny, A.C.Q.M. Vieira, G.C.R.M. Schver, J.L. Soares Sobrinho, P.J. Rolim Neto, P.I. Lee and M.F.R. Soares, *Eur. J. Pharm. Sci.* 119 (2018) 208.
- [9] N.A. Kasim, M. Whitehouse, C. Ramachandran, M. Bermejo, H. Lennernäs, A.S. Hussain, H.E. Junginger, S.A. Stavchansky, K.K. Midha, V.P. Shah and G.L. Amidon, *Mol. Pharm.* 1 (2004) 85.

- [10] L.R.M. Ferraz, A.É.G. Alves, D.D.S.D.S. Nascimento, I.A.E. Amariz, A.S. Ferreira, S.P.M. Costa, L.A. Rolim, Á.A.N Lima and P.J. Rolim Neto, *Acta Trop.* 185 (2018) 127.
- [11] T. Vinuesa, R. Herráez, L. Oliver, E. Elizondo, A. Acarregui, A. Esquisabel, J.L. Pedraz, N. Ventosa, J. Veciana and M. Viñas, *Am. J. Trop. Med. Hyg.* 97 (2017) 1469.
- [12] M.C. Lamas, L. Villaggi, I. Nocito, G. Bassani, D. Leonardi, F. Pascutti, E. Serra and C.J. Salomon, *Int. J. Pharm.* 307 (2006) 239.
- [13] C. Fonseca-Berzal, R. Palmeiro-Roldán, J.A. Escario, S. Torrado, V.J. Arán, S. Torrado- Santiago and A. Gómez-Barrio, *Exp. Parasitol.* 149 (2015) 84.
- [14] A.A. Lima, J.L. Soares-Sobrinho, J.L. Silva, R.A. Corrêa-Júnior, M.A. Lyra, F.L. Santos, B.G. Oliveira, M.Z. Hernandez, L.A. Rolim and P.J. Rolim-Neto, *J. Pharm. Sci.* 100 (2011) 2443.
- [15] D. Leonardi and C.J. Salomon, *J. Pharm. Sci.* 102 (2013) 1016.
- [16] M.C. García, M. Martinelli, N.E. Ponce, L.M. Sanmarco, M.P. Aoki, R.H. Manzo and A.F. Jimenez-Kairuz, *Eur. J. Pharm. Sci.* 120 (2018) 107.
- [17] D. Leonardi, M.E. Bombardiere and C.J. Salomon, *Int. J. Biol. Macromol.* 62 (2013) 543.
- [18] J.L. Soares-Sobrinho, F.L. Santos, M.A. Lyra, L.D. Alves, L.A. Rolim, A.A. Lima, L.C. Nunes, M.F. Soares, P.J. Rolim-Neto and J.J. Torres-Labandeira, *Carbohydr. Polym.* 89 (2012) 323.
- [19] L.C. Sá-Barreto, P.C. Gustmann, F.S. Garcia, F.P. Maximiano, K.M. Novack and M.S. Cunha-Filho, *Pharm. Dev. Technol.* 18 (2013) 1035.
- [20] M.J. Morilla and E.L. Romero. *Adv. Drug Deliver. Rev.* 62 (2010), 576.

- [21] M.J. Morilla, P. Benavidez, M.O. Lopez, L. Bakas and E.L. Romero, *Int. J. Pharm.* 249 (2002) 89.
- [22] M.J. Morilla, P.E. Benavidez, M.O. Lopez and E.L. Romero, *J. Chromatogr. Sci.* 41 (2003) 405.
- [23] M.J. Morilla, J.A. Montanari, M.J. Prieto, M.O. Lopez, P.B. Petray and E.L. Romero, *Int. J. Pharm.* 278 (2004) 311.
- [24] M.J. Morilla, M.J. Prieto and E.L. Romero, *Mem. Inst. Oswaldo Cruz* 100 (2005) 213.
- [25] M.L. Scalise, E.C. Arrúa, M.S. Rial, M.I. Esteva, C.J. Salomon and L.E. Fichera, *Am. J. Trop. Med. Hyg.* 95 (2016) 388.
- [26] M.S. Rial, M.L. Scalise, E.C. Arrúa, M.I. Esteva, C.J. Salomon, L.E. Fichera. *PLoS Negl. Trop. Dis.* 11 (2017) e0006119.
- [27] A.M. Dos Santos-Silva, L.B. de Caland, A.L.C. de S L Oliveira, R.F. de Araújo-Júnior, M.F. Fernandes-Pedrosa, A.M. Cornélio and A.A. da Silva-Júnior, *Mater. Sci. Eng. C Mater. Biol. Appl.* 78 (2017) 978.
- [28] C.J. Salomon, *J. Pharm. Sci.* 101 (2012) 888.
- [29] Chagas Coalition. Breaking the Silence: An Opportunity for Patients with Chagas disease. http://www.coalicionchagas.org/documents/5415804/5524305/breaking+the+silence_report/65091404-85cf-4796-bebb-64c120a26216
- [30] P.A. Sales Junior, I. Molina, S.M. Fonseca Murta, A. Sánchez-Montalvá, F. Salvador, R. Corrêa-Oliveira and C.M. Carneiro, *Am. J. Trop. Med. Hyg.* 97 (2017) 1289.
- [31] A.J. Nunn, *Arch. Dis. Child.* 88 (2003) 369.

- [32] World Health Organization and United Nations Children's Fund. Sources and Prizes of Selected Medicines for Children. 2nd Ed. Geneva: World Health Organization, 2010.
- [33] J. Krämer and H. Blume. Biopharmaceutical aspects of multi-particulates. I. Ghebre-Sellassie (Ed.), Multiparticulate Oral Drug Delivery, Vol. 65, Dekker, New York, 1994, 307.
- [34] K.P. Seremeta, D.A. Chiappetta and A. Sosnik, *Colloids Surf. B Biointerfaces*, 102 (2013) 441.
- [35] C.J. Martínez Rivas, M. Tarhini, W. Badri, K. Miladi, H. Greige-Gerges, Q.A. Nazari, S.A. Galindo Rodríguez, R.Á. Román, H. Fessi and A. Elaissari, *Int. J. Pharm.* 532 (2017) 66.
- [36] K. Adibkia, Y. Javadzadeh, S. Dastmalchi, G. Mohammadi, F.K. Niri and M. Alaei-Beirami, *Colloids Surf. B Biointerfaces* 83 (2011) 155.
- [37] S. Hao, B. Wang, Y. Wang, L. Zhu, B. Wang and T. Guo, *Colloids Surf. B Biointerfaces* 108 (2013) 127.
- [38] A. Akhgari, Z. Heshmati, H. Afrasiabi Garekani, F. Sadeghi, A. Sabbagh, B. Sharif Makhmalzadeh and A. Nokhodchi, *Colloids Surf. B Biointerfaces* 152 (2017) 29.
- [39] L.D. Silva, E.C. Arrúa, D.A. Pereira, C.M. Fraga, T.L. Costa, A. Hemphill, C.J. Salomon and M.C. Vinaud, *Acta Trop.* 161 (2016) 100.
- [40] P. Fonte, P.R. Lino, V. Seabra, A.J. Almeida, S. Reis and B. Sarmiento, *Int. J. Pharm.* 503 (2016) 163.
- [41] Y. Zhang, J. Feng, S.A. McManus, H.D. Lu, K.D. Ristroph, E.J. Cho, E.L. Dobrijevic, H.K. Chan and R.K. Prud'homme, *Mol. Pharm.* 14 (2017) 3480.
- [42] G. Wei, L.F. Lu and W.Y. Lu, *Int. J. Pharm.* 338 (2007) 125.

- [43] T.H. Lee and S.Y. Lin, *Biopolymers* 95 (2011) 785.
- [44] P. Fonte, S. Soares, F. Sousa, A. Costa, V. Seabra, S. Reis and B. Sarmento, *Biomacromolecules* 15 (2014) 3753.
- [45] M. Chacón, J. Molpeceres, L. Berges, M. Guzman and M.R. Aberturas, *Eur. J. Pharm. Sci.* 8 (1999) 99.
- [46] S.R. Kim, M.J. Ho, E. Lee, J.W. Lee, Y.W. Choi and M.J. Kang, *Int. J. Nanomedicine* 10 (2015) 5263.
- [47] R. Katara R and D.K. Majumdar, *Colloids Surf. B Biointerfaces* 103 (2013) 455.
- [48] N. Ubrich, C. Schmidt, R. Bodmeier, M. Hoffman and P. Maincent, *Int. J. Pharm.* 288 (2005) 169.
- [49] M. Gaumet, A. Vargas, R. Gurny and F. Delie, *Eur. J. Pharm. Biopharm.* 69 (2008) 1.
- [50] R. Palmeiro-Roldán, C. Fonseca-Berzal, A. Gómez-Barrio, V.J. Arán, J.A. Escario, S. Torrado-Durán and S. Torrado-Santiago, *Int. J. Pharm.* 472 (2014) 110.
- [51] C. Zhu, Y. Shoji, S. McCray, M. Burke, C.E. Hartman, J.A. Chichester, J. Breit, V. Yusibov, D. Chen and M. Lal, *Pharm. Res.* 31 (2014) 3006.
- [52] S.A. Mahdavi, S.M. Jafari, M. Ghorbani and E. Assadpoor, *Dry. Technol.* 32 (2014) 509.
- [53] C. Anish, A.K. Upadhyay, D. Sehgal and A.K. Panda, *Int. J. Pharm.* 466 (2014) 198.
- [54] N.R. Rabbani and P.C. Seville, *J. Control. Release*, 110 (2005) 130.
- [55] O. Ní Ógáin, L. Tajber, O.I. Corrigan and A.M. Healy, *J. Pharm. Pharmacol.* 64 (2012) 1275.

- [56] A. García, D. Leonardi, G.N. Piccirilli, M.E. Mamprin, A.C. Olivieri and M.C. Lamas, *Drug Dev. Ind. Pharm.* 41 (2015) 244.
- [57] C.P. Reis, R.J. Neufeld, A.J. Ribeiro and F. Veiga, *Nanomedicine* 2 (2006) 8.
- [58] A. Sosnik and K.P. Seremeta, *Adv. Colloid Interface Sci.* 223 (2015) 40.
- [59] K. Bowey, B.E. Swift, L.E. Flynn and R.J. Neufeld, *Drug Dev. Ind. Pharm.* 39 (2013) 457.
- [60] X. Li, N. Anton, C. Arpagaus, F. Belleteix and T.F. Vandamme, *J. Control. Release*, 147 (2010) 304.
- [61] G. Rassu, E. Gavini, G. Spada, P. Giunchedi and S. Marceddu, *Drug Dev. Ind. Pharm.* 34 (2008) 1178.
- [62] C. Sander, K.D. Madsen, B. Hyrup, H.M. Nielsen, J. Rantanen and J. Jacobsen, *Eur. J. Pharm. Biopharm.* 85 (2013) 682.
- [63] W. Khan and N. Kumar, *J. Drug Target.* 19 (2011) 239.
- [64] R. Pignatello, D. Amico, S. Chiechio, C. Spadaro, G. Puglisi and P. Giunchedi, *Drug Deliv.* 8 (2001) 35.
- [65] C.B.M. Figueirêdo, D. Nadvorny, A.C.Q. de Medeiros Vieira, J.L. Soares Sobrinho, P.J. Rolim Neto, P.I. Lee and M.F. de La Roca Soares, *Int. J. Pharm.* 525 (2017) 32.
- [66] W. Abdelwahed, G. Degobert, S. Stainmesse and H. Fessi, *Adv. Drug Deliv. Rev.* 58 (2006) 1688.
- [67] L.H. Reddy, K. Vivek, N. Bakshi and R.S. Murthy, *Pharm. Dev. Technol.* 11 (2006) 167.
- [68] V.V. Pinto, M.J. Ferreira, R. Silva, H.A. Santos, F. Silva and C.M. Pereira, *Colloids Surf. A: Physicochem. Eng. Aspects* 364 (2010) 19.

- [69] D. Quintanar-Guerrero, A. Ganem-Quintanar, E. Allémann, H. Fessi and E. Doelker, *J. Microencapsul* 15 (1998) 107.
- [70] D. Leonardi, C.J. Salomon, M.C. Lamas and A.C. Olivieri, *Int. J. Pharm.* 367 (2009) 140.
- [71] D.R. Paul, *Int. J. Pharm.* 418 (2011) 13.
- [72] M.C. Gohel, M.K. Panchal and V.V. Jogani, *AAPS PharmSciTech.* 1 (2000) E31.
- [73] A. Akbari and J. Wu, *Drug Deliv. Transl. Res.* 7 (2017) 598.
- [74] R. de Oliveira Pedro, S. Hoffmann, S. Pereira, F.M. Goycoolea, C.C. Schmitt and M.G. Neumann, *Eur. J. Pharm. Biopharm.* 131 (2018) 203.

Fig. 1. SEM micrographs of BNZ-loaded particles obtained by spray-drying (A) and freeze-drying (B) and free BNZ (raw material) (C). (A) MP-RS, (B) NP-RS. Scale bar: (A) = 5 μm , (B) = 1 μm , and (C) = 20 μm .

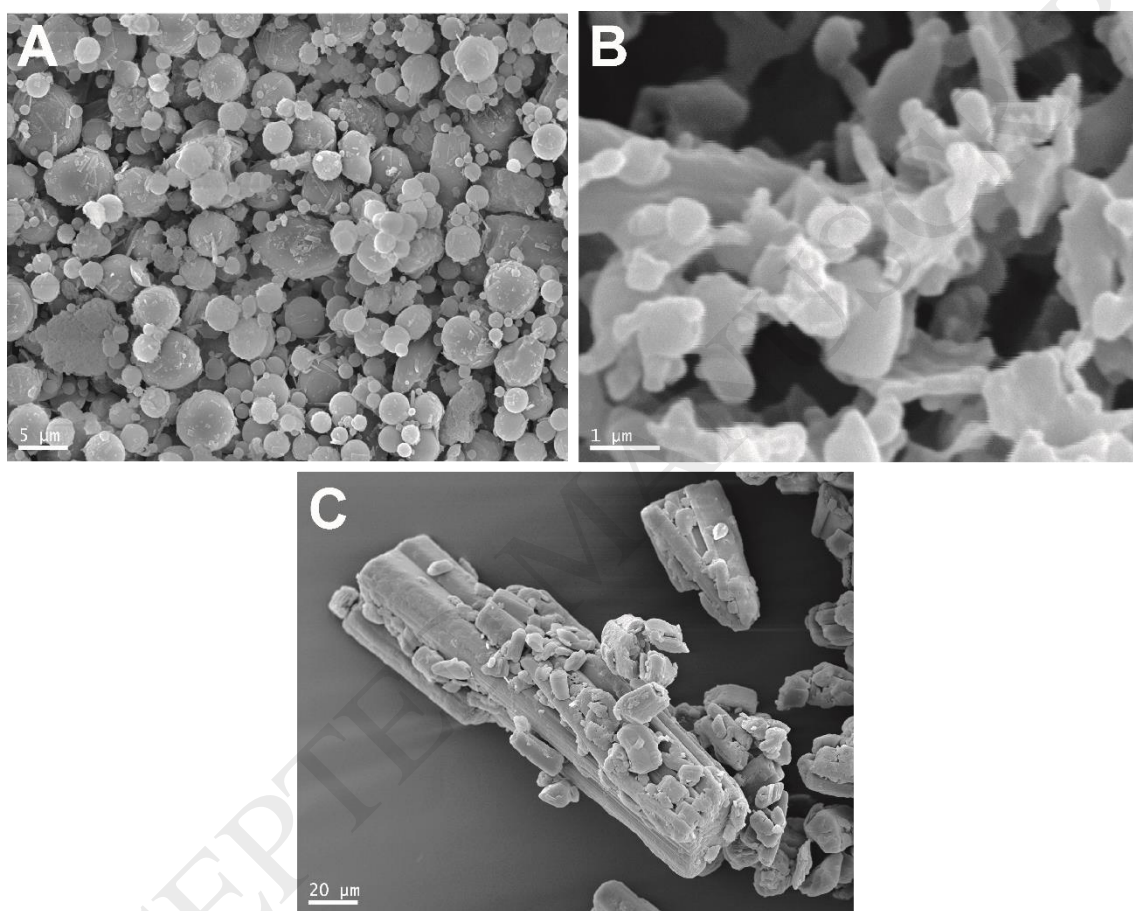


Fig. 2. Stability study of nanoparticles: Particles before (A) and after freeze-drying (B) stored at 25 ± 2 °C; and particles before (C) and after freeze-drying (D) stored at 4 ± 2 °C. *Statistically significant increase of hydrodynamic diameter with respect to initial value ($p < 0.05$).

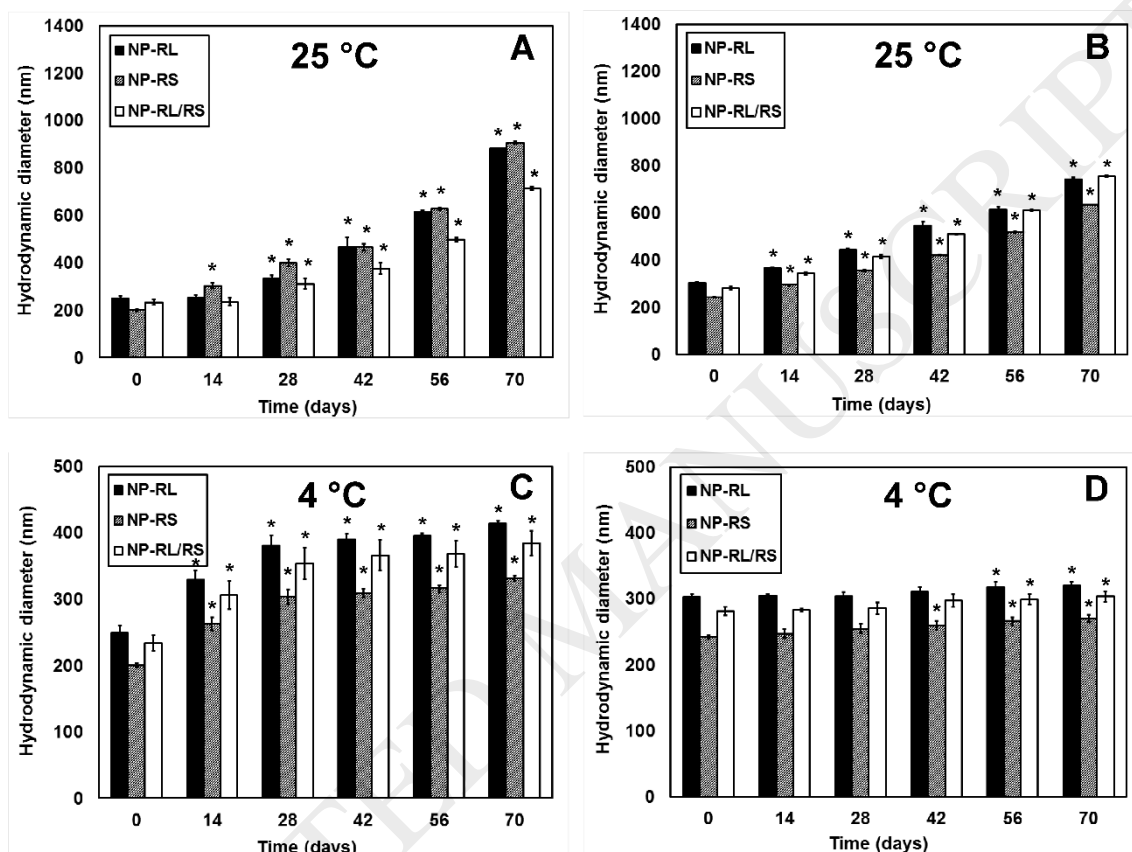
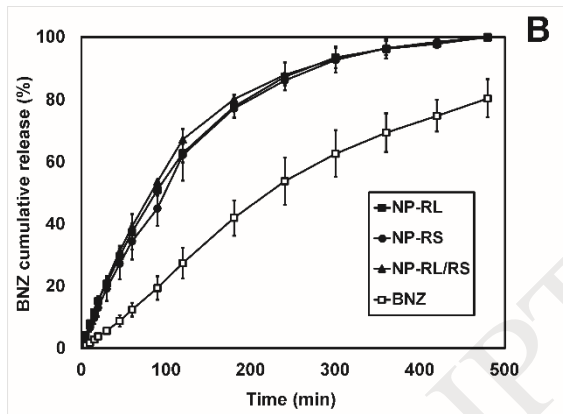
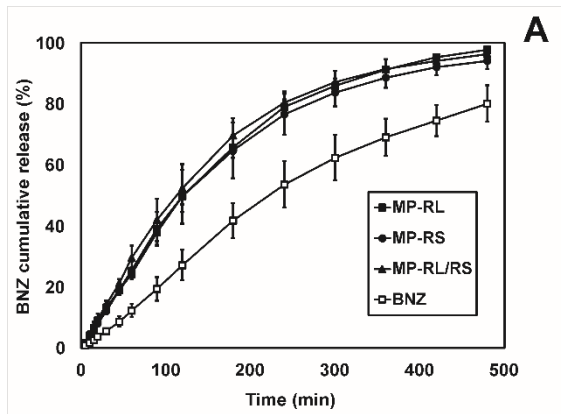


Fig. 3. BNZ cumulative dissolution percentage from polymeric particles obtained by spray-drying (MP-RL, MP-RS and MP-RL/RS) and free BNZ (A) and freeze-drying (NP-RL, NP-RS and NP-RL/RS) and free BNZ (B). Data are reported as mean



ACCEPTED MANUSCRIPT

Formulation	Method of obtaining	%LC ^a (± S.D.)	%EE ^b (± S.D.)	Yield (%) (± S.D.)	Before freeze-drying		
					D _h (nm) ^c (± S.D.)	PDI ^d (± S.D.)	Z-pot (mV) ^e (± S.D.)
NP-RL	Nanoprecipitation/Freeze-drying	17.70 (1.21)	95.16 (2.75)	87.74 (3.31)	249.7 (10.6)	0.096 (0.012)	29.9 (1.5)
NP-RS		17.78 (0.56)	95.97 (2.53)	84.68 (2.12)	200.6 (3.3)	0.099 (0.020)	37.4 (0.9)
NP-RL/RS		17.20 (0.75)	94.40 (4.62)	85.42 (2.04)	233.4 (11.9)	0.103 (0.006)	35.4 (1.7)
MP-RL	Suspension/Spray-drying	24.35 (0.48)	92.64 (1.52)	68.82 (4.22)	-	-	-
MP-RS		23.90 (1.25)	90.96 (2.92)	69.23 (3.46)	-	-	-
MP-RL/RS		20.71 (0.90)	78.81 (0.64)	67.09 (4.33)	-	-	-

Table 1. Properties of the BNZ-loaded particles obtained by different methods and size, size distribution and Z-potential of the particles obtained by nanoprecipitation before and after freeze-drying.

^a %LC, loading capacity.

^b %EE, encapsulation efficiency.

^c D_h, intensity mean hydrodynamic diameter.

^d PDI, polydispersity index.

^e Z-pot, zeta-potential.

^f f_s, factor of variation of the D_h after and before the freeze-drying process.

Sample	T_m (°C) ^a	T_g (°C) ^b	ΔH_m (J/g) ^c	ΔH_g (J/g) ^d	$\%C_{BNZ}$ ^e
BNZ	195	-	118.4	-	100
Eudragit® RL PO	-	50	-	22.8	-
Eudragit® RS PO	-	51	-	27.3	-
NP-RL	195	49	5.1	90.7	24.3
NP-RS	195	49	2.7	30.7	12.8
NP-RL/RS	196	47	0.9	88.7	4.4
MP-RL	197	49	0.3	8.3	1.0
MP-RS	195	49	5.8	36.4	20.5
MP-RL/RS	197	50	0.5	96.3	2.0

Table 2. Thermal analysis of BNZ, polymers and BNZ-loaded particles obtained by freeze-drying and spray-drying.

^a T_m (°C), melting temperature, expressed in °C.

^b T_g (°C), glass transition temperature, expressed in °C.

^c ΔH_m (J/g), enthalpy of melting, expressed in J/g.

^d ΔH_g (J/g), enthalpy of glass transition, expressed in J/g.

^e $\%C_{BNZ}$, crystallinity degree of BNZ, expressed in %.

ACCEPTED MANUSCRIPT

Table 3. Dissolution efficiency values of free BNZ and BNZ-loaded particles and curve fitting analysis.

Formulation	ED ₃₀ ^a	ED ₆₀ ^b	ED ₁₂₀ ^c	Higuchi model		Korsmeyer-Peppas model		
				k_H	R^2_{adj}	k_{KP}	n	R^2_{adj}
BNZ (5 mg)	5.50	12.34	27.21	-	-	-	-	-
NP-RL	20.76*	37.30*	62.60*	5.0288	0.9615	1.7559	0.7016	0.8690
NP-RS	19.04*	34.23*	62.09*	4.9593	0.9575	1.6943	0.7120	0.8569
NP-RL/RS	21.76*	39.07*	67.09*	5.0995	0.9544	1.7585	0.7055	0.8350
MP-RL	13.29*	24.23*	49.78*	4.5486	0.9467	0.7204	0.8500	0.9247
MP-RS	12.02*	25.57*	49.65*	4.4304	0.9458	0.3131	0.9721	0.8526
MP-RL/RS	14.29*	29.55*	52.48*	4.6231	0.9508	0.4084	0.9309	0.8484

^a DE₃₀, dissolution efficiency at t = 30 min.

^b DE₆₀, dissolution efficiency at t = 60 min.

^c DE₁₂₀, dissolution efficiency at t = 120 min.

Higuchi model: k_H , release rate constant.

Korsmeyer-Peppas model: analysis was conducted for $Mt/M^\infty \leq 0.6$; k_{KP} , kinetic constant; n, release exponent.

* Statistically significant increase of ED with respect to free BNZ ($p < 0.001$).